Smith, M., and Khorana, H. G. (1959), *J. Amer. Chem. Soc. 81*, 2911.

Szer, W., and Shugar, D. (1966), *Acta Biochim. Pol. 13*, 177.

Tazawa, I., Tazawa, S., and Ts'o, P. O. P. (1971), 162nd National Meeting of the American Chemical Society, Washington, D. C., Sept, Abstr. BIOL 27.

Ts'o, P. O. P., Schweizer, M. P., and Hollis, D. P. (1969), *Ann. N. Y. Acad. Sci. 158*, 256.

Yamazaki, A., Kumashiro, I., and Takenishi, T. (1968), *Chem. Pharm. Bull. 16*, 338.

Yoshikawa, M., Kato, T., and Takenishi, T. (1967), *Tetrahedron Lett.*, 5056.

Zachau, H. G. (1969), *Angew. Chem., Int. Ed. Engl. 8*, 711.

Zmudzka, B., Janion, C., and Shugar, D. (1969), *Biochem. Biophys. Res. Commun. 37*, 895.

Zmudzka, B., and Shugar, D. (1970), *FEBS (Fed. Eur. Biochem. Soc.) Lett. 8*, 52.

Subunit Interactions and Ligand Binding in Supernatant Malic Dehydrogenase. Cooperative Binding of Reduced Nicotinamide Adenine Dinucleotide Associated with a Monomer–Dimer Equilibrium of the Protein†

M. Cassman* and R. C. King

ABSTRACT: Fluorescence binding studies of reduced nicotinamide adenine dinucleotide (NADH) to S-MDH (supernatant malic dehydrogenase), isolated from beef heart, indicated that the nature of the binding varied with protein concentration. Scatchard plots of NADH titrations showed a curvature convex to the abscissa, characteristic of cooperative binding, at high protein concentrations. With decreasing protein concentration, the Scatchard plots became progressively more linear, approaching the form expected for identical, noninteracting binding sites. The experimental data are consistent with a model assuming a monomer–dimer equilibrium, in which the dimer binds 2 mol of NADH cooperatively. The experimental points were fit by a computer simulation, equating the dimer to the 8×10^4 molecular weight "native" enzyme, and the monomer to the 4×10^4 molecular weight subunit. Ligand binding constants and the monomer–dimer association constant were evaluated from the theoretical model and the best fit to the experimental points. The molar dissociation constant for the monomer–dimer equilibrium was 2.5×10^{-7}, in reasonably good agreement with a directly measured value of 1×10^{-7} obtained from sedimentation equilibrium studies. The results are discussed in relation to previous studies on this enzyme, and in terms of general allosteric control mechanisms. An appendix is included which presents a theoretical evaluation of Scatchard plots obtained from systems demonstrating cooperative binding.

Previous studies on binding of NADH to the supernatant malic dehydrogenase (S-MDH)[1] had provided evidence for a pH- and NADH-dependent transition of the protein (Cassman, 1970). This transition was of particular interest since it occurred over a pH range where an alteration in the kinetic properties of the enzymes had been previously observed (Cassman and Englard, 1966).

In order to clarify the molecular events underlying the NADH-dependent effects, a further investigation was initiated into the nature of the NADH binding. The studies reported here indicate that (a) the protein exists in a monomer–dimer equilibrium, (b) NADH binds to both monomer and dimer, and (c) NADH binds cooperatively to the dimer.

These results are related to previous studies on the enzyme and are also considered in terms of general allosteric control mechanisms.

Materials and Methods

Materials. NADH, oxaloacetate, and D-malate, all of A grade, were obtained from Calbiochem. All other chemicals were standard reagent grade.

Enzyme Purification and Assay. Beef heart supernatant malic dehydrogenase was prepared according to the method of Guha *et al.* (1968). Standard assays were performed in 0.1 M triethanolamine (pH 7.4), using 1×10^{-4} M oxaloacetate and 1×10^{-4} M NADH. Measurements were made at 360 nm, with one unit of enzyme activity defined as a decrease of 0.010 ODU/min. The specific activities were in the range 6.0–8.0 $\times 10^4$ units/min per mg. Protein concentrations were determined by the method of Lowry *et al.* (1951) or from the absorbance at 280 and 260 nm (Layne, 1957). Spectrophotometric measurements were made using a Zeiss PMQ-II spectrophotometer.

Fluorescence Measurements and Calculations. All studies were performed at pH 6.9, in 0.02 M sodium potassium phos-

† From the Section of Biochemistry and Molecular Biology, Department of Biological Sciences, University of California, Santa Barbara, California 93106. *Received May 3, 1972.* This investigation was supported in part by U. S. Public Health Service Grant AM 12681, from the National Institute of Arthritis and Metabolic Diseases.

[1] Abbreviations used are S-MDH, supernatant malic dehydrogenase; *F*, fluorescence; $\bar{\nu}$, average mol of NADH bound per mol of enzyme (8×10^4 molecular weight); *n*, total number of NADH binding sites per mol of enzyme; *j*, Hill coefficient; M_w, weight-average molecular weight. All bracketed symbols denote concentrations.

phate buffer. The concentrations of NADH used in the titrations were determined by measuring the optical densities at 340 nm, and applying the extinction coefficient, $\epsilon^{1\,cm}_{340\,nm}$ 6.22 $\times 10^3$ M^{-1} cm^{-1} (Horecker and Kornberg, 1949). The total volume used was 2 ml. All additions were made using Eppendorf micropipets.

Enzyme preparations used were 70–100% active. Estimates of active enzyme were obtained from measurements of the stoichiometry of NADH binding (see Results). Replicate titrations made over a period of 2 weeks to 1 month were reproducible if corrected for the activity lost by the preparation.

Fluorescence was measured on a Hitachi Perkin-Elmer MPF-2A fluorescence spectrometer, equipped with a thermostated cell holder. The temperature was kept constant at 21–22°, using a circulating water bath. Slit widths on the excitation and emission monochromators were routinely kept at 6 nm. Emission and excitation spectra were uncorrected.

Determinations of NADH–enzyme interactions were made by following either the enhancement of NADH fluorescence at 420 nm, or the quenching of protein fluorescence at 340 nm. (a) The formation of bound NADH was monitored at the 420-nm fluorescence following excitation at 330 nm. Bound NADH was calculated using an equation derived by Laurence (1952).

$$F = F_0 - \int_0^x F_0 dx + \lambda_x \int_0^x F_0 dx$$

where the first term F_0 = calculated fluorescence assuming all the NADH is unbound. The second term represents the fluorescence from free ligand lost through binding, with x = concentration of bound NADH/concentration of total NADH. The third term is the fluorescence generated by the bound ligand, with λ_x = molar fluorescence of bound NADH/molar fluorescence of free NADH, at the wavelength of observation. F_0 was calculated from a standard curve. The standard curve varied by less than 10% over a period of several months.

The most difficult parameter to evaluate was λ_x. This was determined by titrating NADH with enzyme. For a two-site system having association constants K_1 and K_2, a Scatchard plot of the fractional saturation of *ligand* has the form: $\bar{\nu}/[E] = (K_1 + 2[X]K_1K_2) - \bar{\nu}(K_1 + 2[X]K_1K_2)$, where $\bar{\nu}$ = average mol of NADH bound per mol of enzyme, [E] = free enzyme concentration, [X] = free ligand concentration. This can be rearranged in terms of the fluorescence parameters to give

$$\frac{\frac{F}{F_0} - 1}{[E]} = (K_1 + 2[X]K_1K_2)\left\{(\lambda_x - 1) - \left(\frac{F}{F_0} - 1\right)\right\}$$

The term $\lambda_x - 1$ is determined from an extrapolation to the abscissa intercept. In evaluating the limiting slope to obtain this intercept, necessary assumptions are that [X] $\simeq$ 0 and [E] $\simeq$ E total. To ensure the validity of these assumptions, a tenfold range of NADH concentrations were used. The active enzyme concentration in the region of linearity was 0.08–0.8 mg/ml. The value of λ_x once determined remained constant for a given enzyme preparation, independent of changes in the specific activity. Calculated values of λ_x were 51 $\pm$ 2 for the ternary complex with D-malate, and 12 $\pm$ 1 for the binary S-MDH–NADH complex. (b) A separate estimate of NADH binding involved measurement of the quenching of protein fluorescence at 340 nm upon excitation at 280 nm. The experimentally determined maximum quenching was set equal to 100% saturation, and intermediate values were calculated assuming that quenching of protein fluorescence and fractional saturation are linearly related. (The validity of assumption, and of the comparable assumption that λ_x is independent of fractional saturation, will be discussed in Results.) Independent estimates of the concentration of active enzyme, and of the stoichiometry of NADH binding, were required to calculate the concentration of free and bound NADH.

All fluorescence measurements were corrected for dilution and for concentration-dependent nonlinearity of the emission.

Ultracentrifuge Methods. A Spinco Model E analytical ultracentrifuge equipped with an electronic speed control was employed for all sedimentation studies. Equilibrium ultracentrifugation was performed using 30-mm light-path cells fitted with sapphire windows. Column heights of 3-mm were used in these studies. Measurements were made using a Rayleigh optical system and Eastman Kodak II-G spectroscopic plates. The measurements and subsequent data analysis were as previously described (Cassman and King, 1972).

Results

Stoichiometry of NADH–Enzyme Binding. Calculations of the stoichiometry of NADH binding were made assuming a value of 8×10^4 for the molecular weight of S-MDH (Cassman and King, 1972). Fluorescence titrations were performed in the presence of D-malate, which forms a ternary complex with NADH and enzyme. At 420 nm, NADH in the ternary complex has a fluorescence yield approximately fourfold greater than in the enzyme–NADH binary complex. This arises both from an increased quantum yield of NADH in the ternary complex and from a shift in the NADH emission maximum to shorter wavelengths (Cassman and Englard, 1966).

Scatchard plots were obtained from titrations performed at saturating concentrations of D-malate. The abscissa intercept of the limiting slope provides a value for n (NADH binding sites per mol of enzyme) (Scatchard, 1949; Klotz and Hunston, 1971). As can be observed from Figure 1, the nonlinear character of the Scatchard plot limits the range of fractional saturations which can be used in the extrapolation. However, enough points are available in the linear region to allow an accurate estimate of the abscissa intercept. Freshly prepared enzyme gives a value of n = 1.8–2.0/8 $\times 10^4$ g. The precision for any given measurement was $\pm$0.05. Identical values of n were also obtained in the absence of D-malate, with a precision of about $\pm$0.1. These results are in agreement with previous studies indicating that the enzyme is composed of two subunits of identical molecular weight, 3.6–4.0 $\times 10^4$ (Wolfenstein *et al.*, 1968; Gerding and Wolfe, 1969; Cassman and King, 1972).

Since the specific activities of enzyme preparations were observed to decrease upon storage, estimates of active enzyme were periodically made by titrations with NADH in the presence of D-malate. All values of enzyme concentration to be reported were obtained in this manner.

NADH Binding Curves. Titration of 0.08 mg/ml of S-MDH with NADH generated sigmoidal binding curves, which were reflected by Scatchard plots convex to the abscissa (Figure 1). This could be observed in the presence or absence of D-malate. Further studies of the enzyme–NADH binary complex indi-

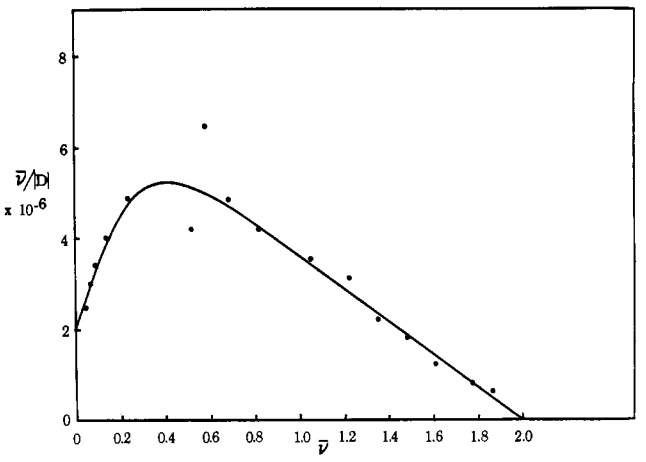

FIGURE 1: A Scatchard plot of the titration of S-MDH with NADH in the presence of D-malate. The initial concentration of enzyme was 1.2×10^{-6} M. D-Malate was present at a concentration of 1×10^{-4} M. In this, as in all subsequent experiments, the buffer used was 0.02 M sodium potassium phosphate (pH 6.9). The titration was performed by following the fluorescence emission of NADH at 420 nm upon excitation at 340 nm.

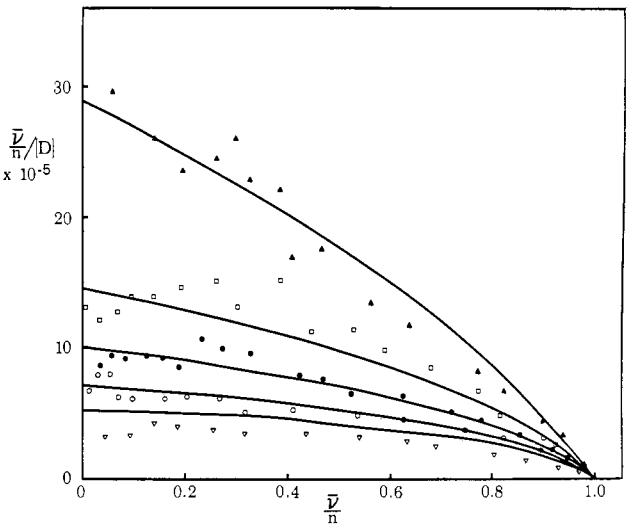

FIGURE 2: Scatchard plots of NADH binding by S-MDH. Titrations with NADH were performed by following either the quenching of protein fluorescence or the enhancement of NADH fluorescence. The symbols represent experimental points obtained at different enzyme concentrations: (▲) 0.01 mg/ml; (□) 0.059 mg/ml; (●) 0.136 mg/ml; (○) 0.292 mg/ml; (▽) 0.567 mg/ml. The solid lines are theoretical curves evaluated at these enzyme concentrations (see Discussion). The abscissa is fractional saturation, $\bar{\nu}/n$. The ordinate is fractional saturation divided by the free NADH concentration.

cated that the form of the binding curves was dependent on the concentration of enzyme. Figure 2 demonstrates that decreasing enzyme concentration leads to progressively more linear Scatchard plots. The titrations were performed by following both NADH and protein fluorescence changes.

The errors in the Scatchard plots largely reflect inaccuracies in determining free NADH concentrations. Measurements of fractional saturation are reproducible to within 5–7%. However, these fluctuations in the values of fractional saturation are much amplified in the calculation of $(\bar{\nu}/n)/[D]$, in regions where the concentration of bound NADH is large relative to the total NADH concentration. [D] represents the molar concentration of free NADH. Thus, the largest errors in the Scatchard plot occur at the maximum ordinate values where [D] is at a minimum. Since the convex shape of the Scatchard plots reflects cooperative binding (see Appendix), the apparent affinity of enzyme for NADH initially increases with increasing fractional saturation. As a consequence, both the position in the Scatchard plot at which the error is greatest, and the magnitude of the error, will be dependent on the degree of cooperativity of the system.

In all measurements, values of fractional saturation markedly deviating from a smooth curve, and titration curves showing marked discontinuities, were discarded. Averaged values were usually taken from two to three duplicate titrations. The points of Figure 2 have a mean deviation in $(\bar{\nu}/n)/[D]$ of about 5% at fractional saturations greater than 0.5. At lower values of fractional saturation, the mean deviations are about 10–20%. At concentrations of enzyme less than 0.008 mg/ml, the Scatchard parameters at fractional saturations below 0.2 cannot be accurately evaluated, due to the very low concentration of free NADH present.

The Hill coefficients, j, obtained from these titration curves are listed in Table I. The highest measured values were 1.3–1.4, obtained from titrations at the highest enzyme concentrations used. With decreasing enzyme concentration, the values of j become progressively smaller. The Hill coefficients are commonly taken to reflect the free energy of interaction between binding sites (Wyman, 1964; Whitehead, 1970), with a system of identical, noninteracting sites having j equal to one. For a two-site system showing cooperative interactions, the maximum value will be two. The values for the Hill coefficients reported in Table I thus indicate positive interactions between binding sites at high enzyme concentrations while the system more closely approximates a set of identical, noninteracting sites as the enzyme concentration decreases.

Fluorescence Yield of Bound NADH as a Function of Enzyme Concentration and Fractional Saturation. The Scatchard plots of Figure 2 have been obtained assuming a proportionality between fluorescence changes and NADH binding which is independent of fractional saturation and of enzyme concentration. This assumption is supported by the identical titration curves generated through the measurement of both protein fluorescence quenching and NADH fluorescence enhancement. A more accurate evaluation of the invariance of fluorescence yield as a function of fractional saturation, at a fixed enzyme concentration, can be obtained by demonstrating the existence of an isoemissive point in the binary com-

TABLE I: Hill Coefficients Obtained at Different Protein Concentrations.[a]

Enzyme Concn (mg ml)	j[b]
0.567	1.37
0.292	1.28
0.136	1.25
0.0588	1.21
0.0097	1.10

[a] The Hill plot of log $(\bar{\nu}/n)[1 - (\bar{\nu}/n)]$ *vs.* $-\log$ [D] was obtained from the experimental points of Figure 2. [b] The slopes of the Hill plots, from which the Hill coefficients are derived, could all be obtained by fitting least-squares straight line to the experimental points. No curvature could be observed. The errors in the measurement of j are ± 0.05.

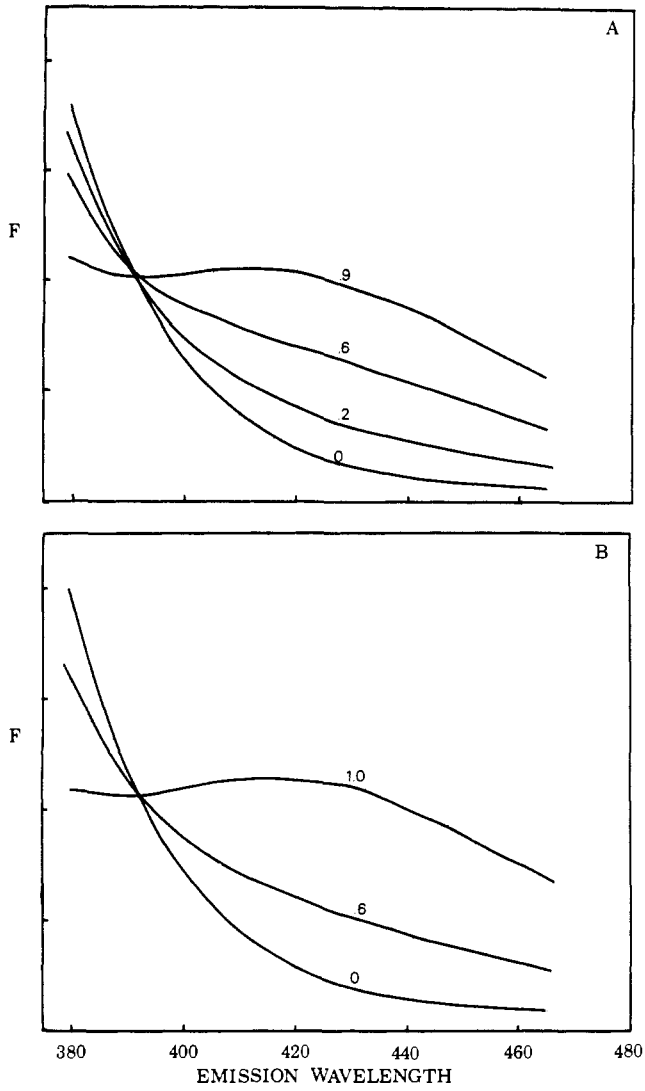

FIGURE 3: Isoemissive point determination at two enzyme concentrations. The excitation wavelength is 280 nm. The abscissa is emission wavelength in nanometers, while the ordinate is the fluorescence given in arbitrary units. The figure presents emission profiles for different degrees of fractional saturation with NADH at (A) 0.292 mg/ml of S-MDH and (B) 0.016 mg/ml of S-MDH. The numbers above each curve give the values of the fractional saturation, $\bar{\nu}/n$.

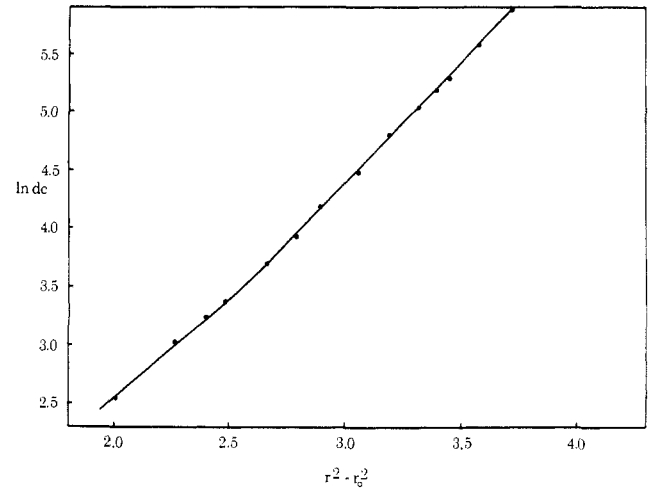

FIGURE 4: Sedimentation equilibrium measurements of S-MDH. The experiment was performed in a 30-mm light-path cell under conditions which left the meniscus depleted of protein. The sample had been extensively dialyzed against 0.02 M sodium potassium phosphate (pH 6.9) + 1% sucrose. The initial protein concentration was 0.5 mg/ml. The equilibrium speed was 22,000 rpm, and the rotor temperature was maintained at 20°. The ordinate gives the logarithm of the concentration expressed in units of micrograms per milliliter. The abscissa is $r^2 - r_0^2$, where r is the distance of the measured point from the center of rotation, and r_0 is the distance of the $c = 0$ point from the center of rotation.

plex fluorescence (Anderson and Weber, 1965). The existence of an isosbestic point in absorption measurements is commonly used as evidence for a two-component system, and the extension of this to fluorescing materials has been developed (Stevens and Ban, 1964; Hamilton and Naqui, 1965).

When an S-MDH–NADH binary complex is excited at 280 nm, an emission profile is observed having a quenched main band emission at 340 nm, and an enhanced long-wavelength emission beyond about 400 nm, relative to the unliganded enzyme. This phenomenon, common to many dehydrogenases (Weber, 1965), is a consequence of a nonradiative energy transfer from the protein chromophores to the nicotinamide ring of the bound NADH. The crossover, or isoemissive point, was followed as a function of fractional saturation at several enzyme concentrations. The enzyme concentrations used attempt to bracket a concentration range over which the apparent cooperativity of NADH binding has altered considerably, as indicated by the degree of curvature of the Scatchard plots and the value of the Hill constants. A small correction (<5%) was made for fluorescence attributable to the direct excitation of NADH. The results indicated the presence of a unique isoemissive point at 395 ± 3 nm (Figure 3). The fluorescent yield is thus independent of fractional saturation and enzyme concentration.

Ultracentrifuge Studies. The dependence of the Scatchard plots on enzyme concentration led us to believe that a protein association–dissociation reaction was occurring. To test this directly, the molecular weight of the unliganded enzyme was examined as a function of protein concentration, using the method of high-speed sedimentation equilibrium. Since previous studies in 12-mm light-path cells showed only a single species of molecular weight 8×10^4 (Cassman and King, 1972), a 30-mm light-path cell was used to extend the measurements to lower protein concentrations. Figure 4 shows the distribution of protein concentration as a function of distance from the center of rotation. The curvature indicates a decreasing molecular weight with decreasing protein concentration. As anticipated, little or no curvature can be observed above a concentration of about 100 μg/ml. This is at the lower limit of accurate measurement in a 12-mm light-path cell. By evaluating the instantaneous slopes of curves such as that of Figure 4, estimates of the molecular weight dependence on protein concentration can be obtained. Values were obtained from experiments using speeds in the range 22,000–28,000 rpm, and concentrations of 0.2–0.7 mg/ml. The molecular weights were identical, with an error of $\pm 3 \times 10^3$ (Figure 5). The reproducibility of the measurements at different rotor speeds and initial protein concentrations indicates that the observed decrease in molecular weight at low concentrations in the cell is due to a reversible equilibrium, rather than to polydispersity (Yphantis, 1964).

Further analysis of the ultracentrifuge data was based on two observations. (1) Studies under dissociating conditions indicated that the enzyme was composed of two subunits of iden-

tical molecular weight, 4×10^4, and (2) a maximum molecular weight of 8×10^4 was observed at concentrations up to 8 mg/ml (Cassman and King, 1972). Sedimentation velocity measurements showed that no further aggregation occurred in the presence of NADH.

The data of Figure 5 were therefore fit to a model assuming a monomer–dimer equilibrium between components of 4×10^4 and 8×10^4 molecular weight. A computer program developed by Dr. Robert Dyson was used (van Holde *et al.*, 1969). The solid line in Figure 5 represents the best fit to the experimental data, and corresponds to a molar dissociation constant of 1×10^{-7}.

Although these results confirm our prediction of a protein–protein interaction, the low degree of dissociation over the concentration range available severely limits the accuracy with which a dissociation constant can be determined. The value of 1×10^{-7} should therefore be considered only as an approximation, with a possible error of as much as two- to threefold.

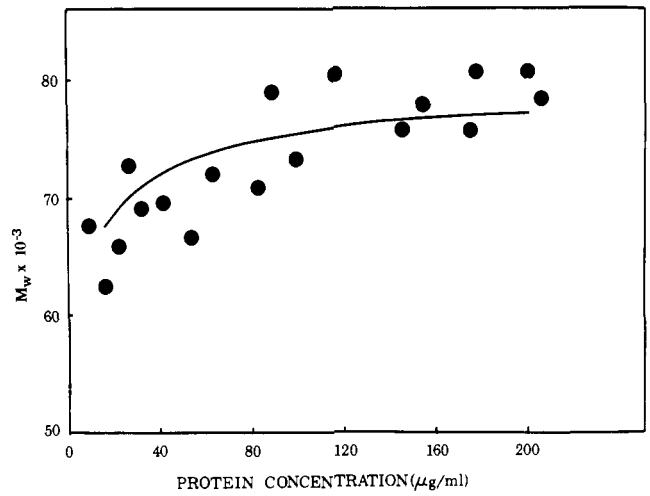

FIGURE 5: Dependence of molecular weight of S-MDH on concentrations. Evaluated from curves such as that of Figure 8, as described in the text. The points are taken from experiments at speeds between 22,000 and 28,000 rpm, and at protein concentrations of 0.2–0.7 mg/ml. The solid line is a theoretical curve for a monomer–dimer equilibrium, obtained as given in the text. The abscissa is the concentration of enzyme in micrograms per milliliter, while the ordinate is the weight-average molecular weight.

Discussion

The fluorescence studies reported in this paper indicate that the S-MDH isolated from beef heart binds 2 mol of NADH/8×10^4 g, and that the nature of this binding is a function of enzyme concentration. The Scatchard plots exhibited increasing curvature with increasing enzyme concentration, the curvature being convex to the abscissa, characteristic of cooperative ligand binding. Further indication of cooperative ligand binding was given by Hill coefficients significantly greater than one, obtained from titration curves at high protein concentrations.

Sedimentation equilibrium studies described here and in a previous publication (Cassman and King, 1972) indicated that (a) the enzyme has a molecular weight of 8×10^4, and is composed of two subunits of identical molecular weight, 4×10^4; (b) aggregates of molecular weight higher than 8×10^4 cannot be observed in the presence or absence of NADH; and (c) dissociation of the enzyme is observable at low enzyme concentrations.

An appropriate model to interpret these observations is that of an enzyme monomer–dimer equilibrium, in which the dimer binds NADH cooperatively. The theoretical monomer is assigned to the 4×10^4 molecular weight subunit. A computer simulation of this model was derived to determine whether a fit could be made to the experimental data. The analysis used a specific mechanistic or configurational (Whitehead, 1970) model, that of Monod *et al.* (1965). However, the choice of this particular model was only for convenience, since the experimental data are not capable of discriminating between this and other mechanistic formulations. Interaction constants will thus be given for the general descriptive system

$$[M] + [D] \rightleftharpoons [MD] \qquad K_b'$$
$$2[M] \rightleftharpoons [M_2] \qquad K_{MD}$$
$$[M_2] + [D] \rightleftharpoons [M_2D] \qquad K_a$$
$$[M_2D] + [D] \rightleftharpoons [M_2D_2] \qquad K_b$$

All the constants are dissociation constants. The parameters K_a, K_b, and K_b' are "intrinsic" binding constants. The word "intrinsic" is put in quotes, since in a system exhibiting cooperative binding the terms describing the interactions are not site-binding constants (Klotz and Hunston, 1971), but may also include isomerization equilibria between conformational states. The equations describing the theoretical model were defined in a form closely analogous to that described by Monod *et al.* (1965), and of Edelstein (1967).

The solid lines in Figure 2 represent the best fit to the experimental points using the model just described. The theoretical parameters used are listed in Table II. The theoretical points for a set of Scatchard plots at different enzyme concentrations are very sensitive to changes in the parameters K_{MD}, K_b, and K_b'. The monomer–dimer dissociation constant, K_{MD}, is primarily responsible for the concentration dependence of the curvature, while the intrinsic dissociation constants K_b and K_b' determine the limiting slopes at high fractional saturations and are the primary determinants of the absolute ordinate values. The assumption is made that $K_b = K_b'$, since the experimental points appear to converge to the same limiting slope at all protein concentrations.

Although the parameters K_{MD}, K_b, and K_b' are restricted to a fairly narrow range of values by the experimental data, the system appears relatively insensitive to K_a, over the enzyme concentration range studied. Increasing K_a above 2.5×10^{-5} (Table II) has little or no effect on the theoretical curves, presumably due to the buffering effect exerted by the monomer–dimer equilibrium.

The theoretical curves provide a good fit to the experimental data with respect to several criteria. (The poor fit at

TABLE II: Theoretical Parameters Used in Fitting the Experiments of Figure 2.

K_{MD}[a]	$2.5 \pm 0.5 \times 10^{-7}$ [b]
K_a	$\geq 2.5 \times 10^{-5}$
K_b	$1.75 \pm 0.2 \times 10^{-7}$

[a] The dissociation constants are defined in the text. [b] The monomer–dimer dissociation constant obtained from ultracentrifuge measurements was 1×10^{-7}.

the highest enzyme concentrations tested is an exception, and will be discussed below.) The ordinate position and the degree of curvature of the Scatchard plots with respect to protein concentration and fractional saturation show similar changes in both the experimental and theoretical curves. Further, an internal check of this model is provided by the independently determined value for the monomer–dimer dissociation constant. The molar dissociation constant obtained using sedimentation equilibrium was 1×10^{-7}, in reasonably good agreement with the curve-fitting value of 2.5×10^{-7}.

There are some indications that the experimental curves exhibit more apparent cooperativity than is generated by our minimal model. This is particularly noticeable in the poor fit of the theoretical curves at the highest concentrations of protein examined. However, in view of the degree of scatter of the experimental points, it did not seem justifiable to introduce more refinements into the model to accommodate these discrepancies. Further modifications would be useful when independent measurements are available to experimentally test the effect of such changes on various parameters of the model, such as monomer–dimer distribution ratios. Tests are currently being performed to determine the optimum conditions for carrying out these measurements.

Qualitatively, systems of the type described have several distinguishing characteristics. The most apparent is, of course, the increased affinity for ligand with decreasing enzyme concentration. Another interesting property is the ability to "buffer" against large changes in the value of K_a. This is demonstrated by the relative invariance of the theoretical Scatchard plots with large changes in K_a, at enzyme concentrations where both monomer and dimer are present. Finally, this system shows a more gradual change in the apparent affinity for ligand as a function of fractional saturation, as compared to a cooperative system which does not undergo an association–dissociation equilibrium. As is shown in the Appendix, in the absence of any dependence of cooperativity on enzyme concentration, a two-site system will always show a maximum in the Scatchard plot. The position and intensity of this maximum are related to the ratio of the two "intrinsic" affinity constants. The superimposition of a monomer–dimer equilibrium results in a buffering with respect to fractional saturation, so that the apparent affinity changes more gradually and between narrower limits.

The coupling of a monomer–polymer equilibrium with allosteric phenomena has been observed in a number of systems. Several distinct classes can be described. The most commonly reported system of this type appears to be that in which the binding of some ligand, together with a change in catalytic properties, is accompanied by an enzyme association–dissociation (Iwatsuki and Okazaki, 1967; Brown and Reichard, 1969). In these cases it is not clear whether the polymerization is required to generate the observed activation or inhibition, or whether it is a secondary consequence of a conformational change accompanying the ligand binding.

A second class has been described by Frieden (1967). In these systems, the cooperativity arises from a differential affinity for ligand of the different polymeric species. Thus, neither the fully associated nor the fully dissociated species will show cooperative interactions, and a reversible equilibrium is a necessary prerequisite for the appearance of allosteric properties. The best characterized example of the class of enzymes is glutamic dehydrogenase (Frieden and Colman, 1967).

In a third class of enzymes, the association equilibrium is between two forms which differ in their allosteric properties. Thus, in S-MDH, the monomer shows normal binding, while the dimer binds NADH cooperatively. Similarly in phosphorylase *b* (Buc and Buc, 1968), a dimer–tetramer association exists, in which the dimer appears cooperative while the tetramer shows Michaelian binding.

The physiological role of these allosteric interactions in S-MDH is far from clear. In part, an interpretation on functional grounds will require a better understanding of the role played by this enzyme *in vivo*. Current hypotheses include (1) the transport of acetyl-CoA from the mitochondrion to the cytoplasm (Lardy *et al.*, 1964); (2) the transport of NADH into and out of the mitochondrion (Krebs *et al.*, 1967); and (3) a participation in gluconeogenesis starting from mitochondrial pyruvate, and coupled to cytoplasmic phosphoenolpyruvate carboxykinase (Marco and Sols, 1969). Although all of these have in common the linkage of intra- and extramitochondrial metabolism, there is no convincing evidence implicating the enzyme in one or another of these processes. Clues to the physiological role of the enzyme, and to the functional significance of the cooperative binding of NADH, may come from studies now under way on allosteric modifiers of the system.

Finally, results reported here may also help in the interpretation of some previously published results. The studies of Cassman and Englard (1966) indicating a stoichiometry of 1 mol of NADH/mol of enzyme was based on a molecular weight of 5.2×10^4 (Englard and Breiger, 1962). This value for the molecular weight is much lower than the subsequently reported estimates of $7.2–8.0 \times 10^4$ (Wolfenstein *et al.*, 1969; Gerding and Wolfe, 1969; Cassman and King, 1972). Examination discloses that all the higher values for the molecular weight were obtained from sedimentation equilibrium measurements, while the value of 5.2×10^4 was determined by combined sedimentation velocity and diffusion. The sedimentation coefficient obtained by Englard and Breiger was 4.6 S, identical with that determined by us for 8×10^4 molecular weight material (Cassman and King, 1972). However, the diffusion coefficient determined by Englard and Breiger was 9.1×10^{-7} cm^2/sec, larger than would be expected for a spherical protein of molecular weight 8.0×10^4 (Tanford, 1961). This high diffusion coefficient is understandable if one assumes that the enzyme was undergoing a rapid monomer–dimer equilibrium. Under these conditions, the boundary spreading would be characteristic of a particle size smaller than 8×10^4, resulting in an anomalously low molecular weight.

Another observation was that of a pH- and NADH-dependent transition in fluorescence and optical rotatory dispersion parameters (Cassman, 1970). Some preliminary experiments (M. Cassman and R. C. King, unpublished results) indicate that the interaction parameters of the allosteric system are strongly pH dependent, showing a marked change over the same pH region as the physical transitions previously noted. One possibility is that the fluorescence and optical rotatory dispersion changes arise from different polymeric and/or conformational species involved in the allosteric transition. Such an observational tool would be especially useful in attempting to unravel the specific allosteric mechanisms involved in the cooperativity.

Appendix

Analysis of ligand binding to macromolecules has been provided by a number of graphical treatments (Klotz, 1953),

among the most important of which is the Scatchard plot (Scatchard, 1949). Klotz and Hunston (1971) have derived the relationship between binding constants and graphical parameters for several graphical methods, including the Scatchard plots, in systems with noninteracting sites. We would like to extend the analysis to cooperative interactions, for macromolecules with two binding sites.

Klotz and Hunston used a model of grouping binding sites into m classes, with n_i the number of sites in class i, and k_i the intrinsic, or site-binding, assiciation constant for that class. The equation describing the dependence of $\bar{\nu}$ on free ligand concentration, [S], is then

$$\bar{\nu} = \sum_{i=1}^{m} \frac{n_i k_i [S]}{1 + k_i [S]} \tag{1}$$

For our purposes, the two-site system can be described by a more general and convenient approach, employing microscopic binding constants

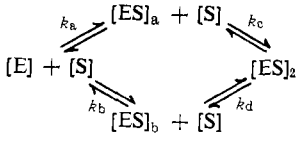

where k_a, k_b, k_c, and k_d are association constants. The expression for $\bar{\nu}$ can be given as

$$\bar{\nu} = \frac{[ES]_a + [ES]_b + 2[ES_2]}{[E] + [ES]_a + [ES_b] + [ES_2]} = \frac{(k_a + k_b)[S] + 2k_a k_c [S]^2}{1 + (k_a + k_b)[S] + k_a k_c [S]^2} \tag{2}$$

This expression will be analyzed in terms of the coordinates of the Scatchard plot, $\bar{\nu}/[S]$ *vs.* $\bar{\nu}$, for four models: (1) identical, noninteracting sites; (2) nonidentical, noninteracting sites; (3) identical sites with negative cooperativity; and (4) identical sites with positive cooperativity. The first two cases will be treated briefly, since they have been adequately described by Klotz and Hunston (1971).

The ordinate of the Scatchard plot can be obtained from eq 2, to give

$$\bar{\nu}/[S] = \{(k_a + k_b) + 2k_a k_c [S]\} - \bar{\nu}\{(k_c + k_b) + k_a k_c [S]\} \tag{3}$$

To obtain the slopes of the Scatchard plot, the first derivative

$$\frac{d(\bar{\nu}/[S])}{d(\bar{\nu})} = \frac{-(k_a + k_b)^2 + 2k_a k_c\{1 - (k_b + k_c)[S] - (k_a k_c)[S]^2\}}{(k_a + k_b) + 4k_a k_c [S] + (k_a + k_b)(k_a k_c)[S]^2} \tag{4}$$

is evaluated for each case.

(1) For identical, noninteracting sites: $k_a = k_b = k_c = k_d = k'$. Substituting this equivalence in eq 4

$$\frac{d(\bar{\nu}/[S])}{d(\bar{\nu})} = -k' \tag{5}$$

Since $[S] \rightarrow 0$, $\bar{\nu} \rightarrow 0$, then from eq 3

$$\lim_{[S]\rightarrow 0} (\bar{\nu}/[S]) = 2k' \text{ (ordinate intercept)} \tag{6}$$

As $[S] \rightarrow \infty$, $\bar{\nu}/[S] \rightarrow 0$, and, from eq 3

$$\lim_{\bar{\nu}/[S]\rightarrow 0} (\bar{\nu}) = 2 \tag{7}$$

Equation 7 gives the value of the abscissa intercept as free ligand goes to infinity. As Klotz and Hunston (1971) have shown, this intercept provides a value for the total number of binding sites. For all the subsequent cases, it will therefore have the value 2.

(2) For nonidentical, noninteracting sites: $k_a = k_d = k_1 > k_b = k_c = k_2$.

$$\lim_{[S]\rightarrow 0} \left(\frac{d(\bar{\nu}/[S])}{d\bar{\nu}}\right) = \frac{k_1^2 + k_2^2}{k_1 + k_2} \tag{8}$$

$$\lim_{[S]\rightarrow \infty} \left(\frac{d(\bar{\nu}/[S])}{d\bar{\nu}}\right) = -\frac{2k_1 k_2}{k_1 + k_2} \tag{9}$$

$$\lim_{[S]\rightarrow 0} (\nu/[S]) = k_1 + k_2 \tag{10}$$

(3) For identical sites with negative cooperativity: $k_a = k_b = k_1 > k_c = k_d = k_2$.

$$\frac{d(\bar{\nu}/[S])}{d(\bar{\nu})} = \frac{k_2 - k_1\{2 + 2k_1[S] + (k_2)^2[S]^2\}}{1 + 2k_2[S] + k_1 k_2 [S]^2} \tag{11}$$

Since $k_2 < k_1$, the slope is always negative.

$$\lim_{[S]\rightarrow 0} \left(\frac{d(\bar{\nu}/[S])}{d(\bar{\nu})}\right) = k_2 - 2k_1 \tag{12}$$

$$\lim_{[S]\rightarrow \infty} \left(\frac{d(\bar{\nu}/[S])}{d(\bar{\nu})}\right) = -k_2 \tag{13}$$

$$\lim_{[S]\rightarrow 0} (\bar{\nu}/[S]) = 2k_1 \tag{14}$$

A comparison of this model with that for nonidentical, noninteracting sites is particularly instructive. For the case where $k_1 \gg k_2$ the association constants for these two models differ only by a constant multiplicative value (Table III). It therefore follows that experimental binding curves can distinguish case 2 from case 3 *only* if k_1 and k_2 are the same order of magnitude.

(4) For identical sites with positive cooperativity: $k_a = k_b = k_1 < k_c = k_d = k_2$. The expression for the first derivative is identical with eq 11. However, since $k_2 > k_1$, the slope is positive at $[S] \rightarrow 0$, and negative at $[S] \rightarrow \infty$. It will go through a maximum when

$$k_2 = k_1\{2 + 2k_2[S] + (k_2)^2[S]^2\} \tag{15}$$

This quadratic can be solved, to give

$$[S] = \frac{-1 \pm \sqrt{k_2/k_1 - 1}}{k_2} \tag{16}$$

Only positive roots need be considered.

TABLE III: Correlation of Graphical Parameters and Binding Constants in the Scatchard Plot.

	Identical Noninteracting (Case 1)	Nonidentical Noninteracting (Case 2)[a]	Identical Negative Cooperativity (Case 3)[a]	Identical Positive Cooperativity (Case 4)[a]
$\lim_{[S]\to 0}\left(\frac{d(\bar{\nu}/[S])}{d(\bar{\nu})}\right)$	$-k'$	$-k_1$	$-2k_1$	k_2
$\lim_{[S]\to \infty}\left(\frac{d(\bar{\nu}/[S])}{d\bar{\nu}}\right)$	$-k'$	$-2k_2$	$-k_2$	$-k_2$
$\lim_{[S]\to 0}(\bar{\nu}/[S])$	$2k'$	k_1	$2k_1$	$2k_1$

[a] Defined for the limiting conditions, where k_1 and k_2 are sufficiently well separated in magnitude.

It should be noted that the Scatchard plot will go through a maxmium, at values of $\bar{\nu} > 0$, when $k_2/k_1 > 2$. The position of the maximum and its ordinate value can be obtained by substituting the calculated value of [S] from eq 16 into eq 2 and 3.

Finally, the equations for the slopes and the ordinate intercept are identical with those given in eq 12–14. In the limit, where $k_2 \gg k_1$, the correspondence between the graphical parameters and the binding constants are given in Table III.

References

Anderson, S. R., and Weber, G. (1965), *Biochemistry 4*, 1948.

Brown, N. C., and Reichard, P. (1969), *J. Mol. Biol. 46*, 25.

Buc, M. H., and Buc, H. (1968), *in* The Regulation of Enzyme Activity and Allosteric Interactions, Kvamme, E., and Pihl, A., Ed., New York, N. Y., Academic Press, p 109.

Cassman, M. (1970), *J. Biol. Chem. 242*, 2013.

Cassman, M., and Englard, S. (1966), *J. Biol. Chem. 241*, 287.

Cassman, M., and King, R. C. (1972), *Biochim. Biophys. Acta 257*, 135.

Edelstein, S. J. (1967), Ph.D. Thesis, University of California, Berkeley, Calif.

Englard, S., and Breiger, H. H. (1962), *Biochim. Biophys. Acta 56*, 571.

Frieden, C. (1967), *J. Biol. Chem. 242*, 4045.

Frieden, C., and Colman, R. F. (1967), *J. Biol. Chem. 242*, 1705.

Gerding, R. K., and Wolfe, R. G. (1969), *J. Biol. Chem. 244*, 1164.

Guha, A., Englard, S., and Listowsky, I. (1968), *J. Biol. Chem. 243*, 609.

Hamilton, T. D. S., and Naqui, K. R. (1965), *Chem. Phys. Lett. 2*, 374.

Horecker, B. L., and Kornberg, A. (1949), *J. Biol. Chem. 175*, 385.

Iwatsuki, N., and Okazaki, R. (1967), *J. Mol. Biol. 29*, 139.

Klotz, I. M. (1953), *Proteins 2*, Chapter 8.

Klotz, I. M., and Hunston, D. L. (1971), *Biochemistry 10*, 3065.

Krebs, H. A., Gascoyne, T., and Notton, B. M. (1967), *Biochem. J. 105*, 275.

Lardy, H. A., Shrago, E., Young, W., and Paetku, V. (1964), *Science 144*, 564.

Laurence, D. J. R. (1952), *Biochem. J. 51*, 168.

Layne, E. (1957), *Methods Enzymol. 3*, 454.

Lowry, O. H., Rosebrough, N. J., Farr, A. L., and Randall, R. J. (1951), *J. Biol. Chem. 193*, 265.

Marco, R., and Sols, A. (1969), *Fed. Eur. Biochem. Soc. Symp. 19*, 63.

Monod, J., Wyman, J., and Changeux, J.-P. (1965), *J. Mol. Biol. 12*, 68.

Scatchard, G. (1949), *Ann. N. Y. Acad. Sci. 51*, 660.

Stevens, B., and Ban, M. I. (1964), *Trans. Faraday Soc. 60*, 1515.

Tanford, C. (1961), Physical Chemistry of Macromolecules, New York, N. Y., Wiley.

van Holde, K. E., Rossetti, G. P., and Dyson, R. D. (1969), *Ann. N. Y. Acad. Sci. 164*, 279.

Weber, G. (1965), *Proteins 3*, 445.

Whitehead, E. (1970), *Progr. Biophys. Mol. Biol. 20*, 321.

Wolfenstein, C., Englard, S., and Listowsky, I. (1968), *J. Biol. Chem. 243*, 609.

Wyman, J. (1964), *Advan. Protein Chem. 19*, 223.

Yphantis, D. A. (1964), *Biochemistry 3*, 297.